

Off-center instability in $\text{SrCl}_2:\text{Fe}^+$: Role of unoccupied $4p$ orbitals

P. García-Fernández,¹ J. A. Aramburu,¹ M. T. Barriuso,² and M. Moreno¹

¹*Departamento de Ciencias de la Tierra y Física de la Materia Condensada, Universidad de Cantabria, Avenida de los Castros s/n, 39005 Santander, Spain*

²*Departamento de Física Moderna, Universidad de Cantabria, Avenida de los Castros s/n, 39005 Santander, Spain*
(Received 4 November 2005; revised manuscript received 22 February 2006; published 23 May 2006)

Recent electron nuclear double resonance experiments on the $\text{Fe}(\text{II})$ center in $\text{SrCl}_2:\text{Fe}^+$ have unambiguously demonstrated that an isolated Fe^+ impurity (without any close defect) undergoes a big off-center motion along $\langle 001 \rangle$ type directions. As Fe^+ in SrCl_2 exhibits a high spin value $S=3/2$, its ground state in a perfect cubal symmetry would be ${}^4A_2 (e_g^4 t_{2g}^3)$ with no orbital degeneracy, a situation which is thus different than that for d^9 and d^4 ions in fluorite-type lattices. Density functional theory (DFT) calculations carried out on clusters involving up to 51 atoms confirm that the instability of Fe^+ is spontaneous. It is found that Fe^+ performs a big excursion of 1.3 Å from the center of the FeCl_6^{7-} cube to a position close to the center of a $\{001\}$ face. Despite this huge distortion, the associated well depth is found to be only 0.28 eV, so indicating the subtle origin of the instability. At a variance with what happens for Jahn-Teller distortions, off-center displacements cannot be understood by looking only to the half-filled t_{2g} antibonding orbitals, which are related from the beginning to the modifications of involved wave functions as described by the pseudo-Jahn-Teller theory. The polarization of the electronic cloud through admixtures of $3d(\text{Fe}^+)$ orbitals with deep fully occupied $3p(\text{Cl}^-)$ as well as unoccupied $4p(\text{Fe}^+)$ orbitals is found to play a key role, while the electrostatic field of the rest of the lattice acts against the distortion. Results obtained for different electronic configurations support these conclusions. Wave-function-based complete active space second-order perturbation theory calculations have also been carried out. At a variance with the DFT results, such calculations are unable to reproduce the subtle off-center instability.

DOI: [10.1103/PhysRevB.73.184122](https://doi.org/10.1103/PhysRevB.73.184122)

PACS number(s): 61.72.Bb, 71.15.Mb, 71.70.Ej, 31.15.Ar

I. INTRODUCTION

Very often an impurity, M , entering an insulating AX_p lattice, occupies an on-center position substituting the host lattice cation A . However, in some special cases, the on-center position is unstable and the impurity is found to undergo a spontaneous off-center displacement,¹⁻¹³ which can involve distances larger than ~ 1 Å. Therefore, off-center instabilities can produce drastic changes of local geometry, and thus of all properties associated with the impurity. Off-center impurities have been used as model objects for the investigation of the tunnel movement of atomic particles and quantum diffusion mechanisms in a solid state.¹³⁻¹⁸ The study of impurities with an off-center instability is also of interest in the realm of phase transitions in pure compounds and, in particular, of those involving the ordering of local dipole moments. In fact, in a doped cubic lattice, an off-center motion of the impurity leads to the appearance of a local dipole moment, a situation that resembles, but partially, that encountered in a ferroelectric material.¹⁹⁻²² Off-center displacements of atoms are also found in several molecules of chemical and biochemical interest as, for example, metal porphyrins and hemoproteins.²⁰

Magnetic resonance measurements^{1-3,5,6,8-12} and density functional theory (DFT) calculations^{23,24} have unambiguously demonstrated the existence of off-center instabilities in some fluorite-type lattices doped with Jahn-Teller d^9 and d^4 ions. This behavior has been proved experimentally for Cu^{2+} , Ag^{2+} , Ni^+ , and Cr^{2+} ions in SrCl_2 . However, in the CaF_2 host lattice Cu^{2+} , Ag^{2+} , and Cr^{2+} remain on center,^{25,26} while only the Ni^+ impurity is clearly located off center.^{5,23} In all these cases, when the instability is taking place, the off-center mo-

tion is always found to be along the $\langle 100 \rangle$ directions leading to a local C_{4v} symmetry. This is reasonable, since for a lattice with a fluorite structure, the smallest Born-Mayer repulsion from neighbor halide anions is expected when the impurity M goes along the $\langle 100 \rangle$ directions.

Very recently, electron paramagnetic resonance²⁷ (EPR) and specially electron nuclear double resonance²⁸ (ENDOR) spectra carried out on the so-called $\text{Fe}^+(\text{II})$ center in SrCl_2 demonstrate that the Fe^+ impurity is not at the Sr^{2+} site but surrounded by *only* four Cl^- ions of a $\langle 001 \rangle$ face (Fig. 1). Moreover, such experimental data do not provide any evidence on an associated defect, that could be responsible for the off-center displacement of Fe^+ . Therefore, the instability observed for the $\text{Fe}^+(\text{II})$ center in SrCl_2 appears to have an intrinsic origin.

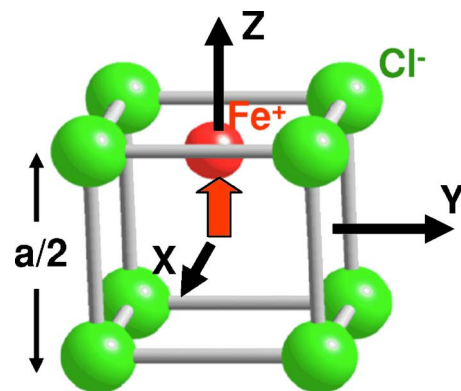


FIG. 1. (Color online) Picture of the off-center motion of Fe^+ in the SrCl_2 lattice.

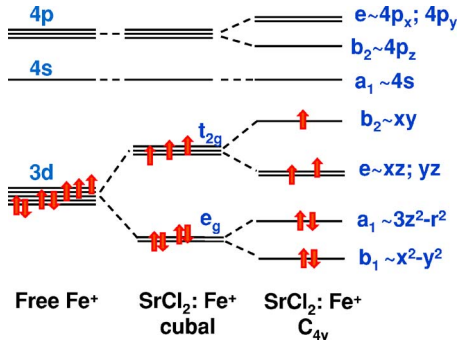


FIG. 2. (Color online) Level scheme of the mainly 3d, 4s, and 4p orbitals of Fe for the $\text{SrCl}_2:\text{Fe}^+$ center for the cubal reference (O_h) and C_{4v} geometries.

It is worth noting that, although the expected ground state of Fe^+ in cubal symmetry is ${}^4A_{2g}(e_g^4 t_{2g}^3)$ (Fig. 2), however, available EPR spectra²⁷ are *fitted* using an effective spin $S' = 1/2$. This seemingly puzzling situation can be understood considering that EPR measurements are carried out²⁷ at the equilibrium geometry (Fig. 1) displaying a local C_{4v} symmetry. Under C_{4v} symmetry, a zero-field splitting term is allowed, which produces the separation of the two $|3/2; \pm 1/2\rangle$ and $|3/2; \pm 3/2\rangle$ Kramers doublets. When the distortion is strong enough, the energy of an EPR transition like $|3/2; 1/2\rangle \rightarrow |3/2; 3/2\rangle$ can be higher than the microwave photon energy, and thus, it cannot be observed. Therefore, in this case, *only* the $|3/2; -1/2\rangle \rightarrow |3/2; 1/2\rangle$ transition can be well detected under an applied magnetic field, \mathbf{H} . Bearing in mind that $\langle 3/2; -1/2 | S_x | 3/2; 1/2 \rangle = \hbar$, it turns out that when \mathbf{H} is perpendicular to the principal axis of the distortion, then $g'_\perp = 2g_\perp$, where g_\perp is the actual gyromagnetic factor corresponding to a $S=3/2$ ground state. Thus, the measured value²⁷ $g'_\perp = 5.2$ for the $\text{Fe}^+(\text{II})$ center in SrCl_2 , supports a ground state with $S=3/2$ rather than with $S=1/2$. A similar situation has been encountered for Fe^{3+} ions in strong tetragonal or orthorhombic fields.²⁹

The strong off-center motion observed for an *isolated* Fe^+ ion in SrCl_2 is, in principle, a little surprising because there is *not* any orbital degeneracy in the ${}^4A_{2g}(e_g^4 t_{2g}^3)$ ground state. Therefore, this situation is opposite to that for d^9 or d^4 ions where the ground state in cubal symmetry [${}^2T_{2g}(e_g^4 t_{2g}^5)$ and ${}^5T_{2g}(e_g^2 t_{2g}^5)$, respectively] does exhibit such a degeneracy. The present work is addressed to gain better insight into this problem paying particular attention to the mechanisms responsible for the off-center instability in $\text{SrCl}_2:\text{Fe}^+$. For this reason, the implications of this research are not only of interest for understanding the behavior of impurities in insulators, but also of interest in the realm of ferroelectric and incipient ferroelectric materials.^{20–22}

For achieving this goal, *ab initio* total energy calculations of the ground state in the DFT framework have been performed. For exploring the existence of a spontaneous off-center instability at $T=0$ K, the ground-state energy, $E(Z)$, has been computed placing the Fe^+ impurity at different $(0, 0, Z)$ positions and for different electronic configurations. Recently, this kind of calculation has been a big help for clarifying the origin of the off-center instability observed for

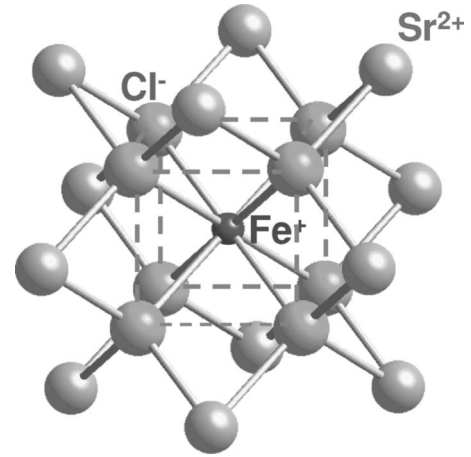


FIG. 3. Cluster of 21 ions $\text{FeCl}_8\text{Sr}_{12}^{15+}$, used to simulate the $\text{SrCl}_2:\text{Fe}^+$ center.

some systems involving a d^9 ion in a lattice with a fluorite structure.^{23,24} As in the present work emphasis is put on the role of *different orbitals* on the off-center instability, self-consistent charge-extended Hückel (SCCEH) calculations have also been carried out. In these simpler calculations, it becomes possible to easily suppress a given orbital from the basis set, and thus, to study its *influence* on the final result. This procedure has been applied to explain the origin of the sensitivity shown by the cubic field splitting parameter, $10Dq$, to changes of the metal-ligand distance.³⁰

For the sake of completeness, highly correlated wavefunction-based complete active space second-order perturbation theory (CASPT2) calculations have also been carried out for the present system. This allows us to compare their results with those obtained through the DFT approach toward a challenging problem, which is very subtle indeed.

II. COMPUTATIONAL DETAILS

DFT calculations for the $\text{SrCl}_2:\text{Fe}^+$ center have been carried out on clusters centered at the Fe^+ impurity. Previous results^{23,24} obtained for Ni^+ - and Cu^{2+} -doped MF_2 ($M = \text{Ca}, \text{Sr}$) and SrCl_2 showed that the off-center motion is well reproduced by a cluster containing only 21 atoms (Fig. 3), because the active 3d electrons are localized in the region formed by the impurity and ligands. Moreover, calculations carried out for clusters involving up to 51 atoms did not significantly improve the results derived on the 21-atom cluster for $\text{SrCl}_2:\text{Fe}^+$. Calculations have been performed for clusters *in vacuo* as the electrostatic potential due to the rest of the lattice on the cluster region is found to be very flat in these systems.

Results presented in the next section have been obtained by means of the Amsterdam density functional (ADF) program³¹ using the Vosko-Wilk-Nusair exchange-correlation functional³² for the local density approximation (LDA). Similar results were obtained using the generalized gradient approximation (GGA) in its Becke-Lee-Yang-Parr (BLYP) form.³³ The employed basis sets consists of three Slater-type orbitals (STOs) plus a polarization function per atomic or-

bital as implemented in the ADF program. Use was made of the larger frozen core available in the database as these orbitals play only a minor role in the studied properties. As a salient feature, calculations have also been performed on *other* electronic configurations different from $a_1(3z^2 - r^2)^2 b_1(x^2 - y^2)^2 e(xz, yz)^2 b_2(xy)^1$ corresponding to the ground state in C_{4v} symmetry. This kind of calculation where the seven valence electrons from Fe^+ are placed in a different way, provide relevant information on the mechanisms responsible for the instability. For carrying out these processes, each orbital obtained in the calculations is easily identified by its symmetry label, energy, as well as through the usual population analysis. It is worth noting that in the usual Kohn-Sham (KS) DFT calculations, the electronic density is represented by only one Slater determinant (constructed with an orbitals solution of the one-electron KS equations),³⁴ and thus, the corresponding wave function describes a state that is orbitally singlet. This means that the 4B_1 state of the $a_1(3z^2 - r^2)^2 b_1(x^2 - y^2)^2 e(xz, yz)^2 b_2(xy)^1$ configuration (in C_{4v} symmetry) can easily be calculated through the DFT. A more complex process is required for calculating general multiplet states in the framework of the DFT.³⁵⁻³⁷

In order to be sure about the obtained LDA and GGA results, some calculations were also carried out using the three parameter hybrid semiempirical B3LYP functional³⁸ implemented in the GAUSSIAN 98 package.³⁹ These calculations use the double zeta LANL2DZ basis, which employ Gaussian-type orbitals (GTOs) and pseudopotentials to simulate the core electrons. The obtained results for the ground state are similar to the corresponding LDA and GGA values, while it was not possible to converge the calculations for other configurations.

As pointed out in the Introduction, CASPT2 calculations on the $\text{SrCl}_2:\text{Fe}^+$ system have also been performed. CASPT2 is an accurate *ab initio* wave-function-based methodology⁴⁰⁻⁴² that has been successfully employed in the study of different solid-state problems.⁴³ It includes most of the electronic correlation effects combining two strategies. In the first step, an important part of the correlation is treated in a variational way by constructing an accurate wave function where all possible Slater determinants corresponding to a chosen active space are included. An active space containing seven electrons distributed in all possible ways over the five $3d$ orbitals of Fe was considered. Moreover, some calculations have also been performed including the $4s$ and $4p$ orbitals of Fe in the active space. In the second step, the remaining (mostly dynamical) electron correlation effects are included by the many-body second-order perturbation theory in which all valence electrons are correlated. Because of the high computational cost of this kind of calculations it was not possible to include, in the active space, the electrons lying in bonding orbitals.

Some semiempirical SCCEH calculations have also been performed in order to study the effect of the removal of some orbitals from the basis set on the off-center instability. More details about this method can be found in Ref. 44.

III. RESULTS AND DISCUSSION

In the first step, the ground state of Fe^+ in SrCl_2 in an on-center cubal position has been calculated. DFT calcula-

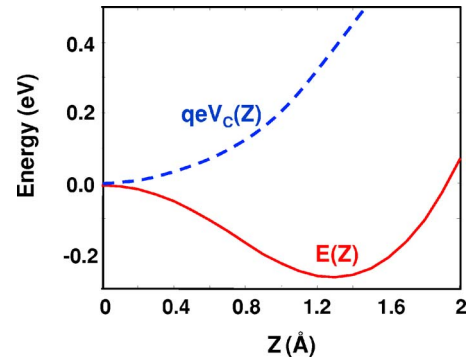


FIG. 4. (Color online) Solid line: Ground-state DFT total energy, $E(Z)$, of $\text{SrCl}_2:\text{Fe}^+$ calculated for different values of the Z coordinate. Dashed line: Simple model representing the barrier, $qeV_C(Z)$, for moving a nondeformable Fe^+ ion with the total charge qe through the potential, $V_C(Z)$, generated by point charges located at lattice sites.

tions confirm that the energy of the $^4A_{2g}(e_g^4 t_{2g}^3)$ state is lower than the corresponding energy for a $S=1/2$ configuration. Moreover, it is also found in the DFT calculations that the ground state has $S=3/2$ even if Fe^+ is placed at $(0, 0, Z)$ and $Z \approx a/4$ (Fig. 1), while the lowest excited state with $S=1/2$ is lying about 1 eV above the ground state. The ground state corresponds to a $a_1(3z^2 - r^2)^2 b_1(x^2 - y^2)^2 e(xz, yz)^2 b_2(xy)^1$ configuration, the $b_2(xy)$ level lying ~ 1 eV above $e(xz, yz)$, which is very close to $b_1(x^2 - y^2)$ and $a_1(3z^2 - r^2)$ orbitals. It is worth noting that in the $^4A_{2g}$ ground state, only the unpaired electron residing on the $b_2(xy)$ orbital is responsible for the isotropic superhyperfine constant experimentally well detected.^{27,28} Indeed, the overlap of an xz wave function of free Fe^+ with $3s$ wave functions of four top Cl^- ligands in Fig. 1 is rigorously zero when $Z=a/4$. By contrast, the $b_2(xy)$ level would be empty if the ground state has $S=1/2$.

According to previous works on the off-center instability of d^9 impurities,^{23,24} the geometry optimization of the 21-atom cluster has been performed following a two-step procedure. In the first step, the equilibrium impurity-ligand distance for Fe^+ in SrCl_2 , R_{ML} , has been calculated imposing a cubal geometry. As expected, the obtained value $R_{\text{ML}} = 2.92 \text{ \AA}$ is a little higher than $R_{\text{ML}} = 2.82 \text{ \AA}$ derived²⁴ for the divalent Cu^{2+} impurity in the same lattice. In the second step, the d^7 impurity has been allowed to move along the $[001]$ direction, relaxing the top and bottom ligands at the same time. A plot of the ground-state total energy calculated at different $(0, 0, Z)$ points, $E(Z)$, of $\text{SrCl}_2:\text{Fe}^+$ is reported in Fig. 4. In that figure, the calculated Coulomb barrier, $qeV_C(Z)$, for moving a nondeformable Fe^+ ion with a total charge qe (e =proton charge) along the $[001]$ direction, is also shown. In this calculation, a value of $q = +0.66$ corresponding to the initial on-center position was used. As recently pointed out,^{23,24} this Coulomb barrier acts against an off-center motion that occurs only through the deformation of the electronic density, and thus, it produces changes of bonding.

It is worth noting in Fig. 4 that the calculated derivative of $E(Z)$ at $Z=0$ is null. This result comes from the lack of linear vibronic coupling between the $^2T_{2g}(e_g^4 t_{2g}^3)$ ground state in the

cubic symmetry and the t_{1u} vibrational mode. In fact, within the vibronic theory,²⁰ the behavior *around* the initial high-symmetry geometry can be explored through the Hamiltonian, H , briefly expressed as

$$H = H_0 + V_{\Gamma\gamma}(\mathbf{r})Q_{\Gamma\gamma}. \quad (1)$$

Here, H_0 represents the Hamiltonian describing the electronic states when the Fe^+ nucleus is at the center of the cube formed by the ligands. The second term depicts the linear vibronic interaction involving general distortion coordinates designated by $Q_{\Gamma\gamma}$, where Γ is the corresponding irreducible representation, their rows being denoted by γ . Let us denote by $|\Psi_{n;j}^0\rangle$ the wave functions corresponding to the ground ($n=0$) and excited states ($n \geq 1$) of the unperturbed Hamiltonian, H_0 , where the index j reflects the possible degeneracy. In the present case, H_0 is invariant under the inversion center operation, and so we obtain $\langle \Psi_0^0 | V_{\Gamma\gamma} | \Psi_0^0 \rangle = 0$ for $\Gamma = T_{1u}$ and $\gamma = X, Y, Z$.

Thus, this situation is quite different from the situation found in the $E \otimes e$ Jahn-Teller problem²⁰ where the equilibrium geometry and the Jahn-Teller energy (but not the barrier among equivalent minima) is determined *only* by the matrix element $\langle \Psi_{0;\theta}^0 | V_{\Gamma,\theta}(\mathbf{r}) | \Psi_{0;\theta}^0 \rangle = -\langle \Psi_{0;\varepsilon}^0 | V_{\Gamma,\theta}(\mathbf{r}) | \Psi_{0;\varepsilon}^0 \rangle$ ($\Gamma = E_g$; $\theta = 3z^2 - r^2$, $\varepsilon = x^2 - y^2$) involving the *frozen* wave functions $|\Psi_{0;\theta}^0\rangle$ and $|\Psi_{0;\varepsilon}^0\rangle$.

For this reason, the behavior of $E(Z)$ around $Z=0$ can only be explained by the admixture of the *odd* excited states of H_0 into the ground states due to vibronic coupling with the t_{1u} mode. The bonding between Fe^+ and close anions is inevitably modified (rebonding effects) by this admixture, *even at the beginning* of the distortion. Associated with this admixture there is a second-order correction to the ground-state energy, ΔE_0 , given by

$$\Delta E_0 = - \sum_n \frac{|\langle \Psi_0^0 | V_{T_{1u}Z}(\mathbf{r}) | \Psi_n^0 \rangle|^2}{E_n - E_0} Z^2 = - \frac{1}{2} K_v Z^2. \quad (2)$$

This pseudo-Jahn-Teller mechanism produces a softening of the ground-state force constant, which, thus, is in competition with the positive force constant²⁰

$$K_0 = \langle \Psi_0^0 | \frac{\partial^2 H_0}{\partial Z^2} | \Psi_0^0 \rangle \quad (3)$$

involving only the ground-state *frozen* wave function $|\Psi_0^0\rangle$. When $K_0 < K_v$, the instability comes out, and the curvature of $E(Q_\Gamma)$ at $Q_\Gamma=0$ becomes negative.

The plot of the calculated $E(Z)$ values for $\text{SrCl}_2:\text{Fe}^+$ (Fig. 4) clearly shows that the curvature $[\partial^2 E(Z)/\partial Z^2]_{Z=0}$ at the origin is certainly negative. Thus, this fact is consistent with the existence of a spontaneous *intrinsic* off-center instability for a substitutional Fe^+ ion in the SrCl_2 lattice. The minimum of the $E(Z)$ curve is found at $Z_0=1.31 \text{ \AA}$ implying a big displacement of Fe^+ from the on-center position. This distortion is not sufficiently big for Fe^+ to reach the plane formed by the four top Cl^- ions in Fig. 1 located at $Z_p=1.74 \text{ \AA}$. Thus, the existence of a big off-center displacement in $\text{SrCl}_2:\text{Fe}^+$ is in agreement with the recent EPR (Ref. 27) and

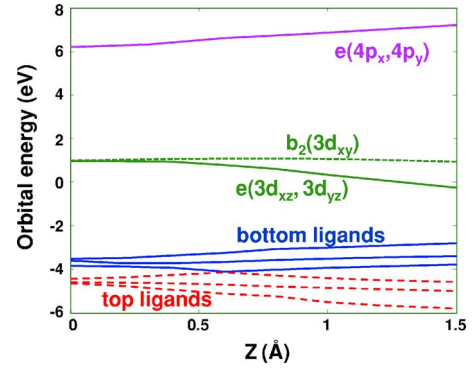


FIG. 5. (Color online) Energy profiles obtained from DFT calculations for the relevant orbitals of $\text{SrCl}_2:\text{Fe}^+$.

ENDOR (Ref. 28) data from which a value $Z_0=1.65 \text{ \AA}$ has been estimated.

Calculations using the CASPT2 methodology have also been carried out. While DFT calculations are able to reproduce the off-center motion in $\text{SrCl}_2:\text{Fe}^+$, the much more computationally expensive attempts using the CASPT2 method have all been unsuccessful. Relevant conclusions about this surprising fact will be shown in Sec. IV.

Here, it should be noted that although the big excursion of Fe^+ in SrCl_2 leads to important changes of many observable properties, the energy difference between the on-center and the off-center position is only 0.28 eV according to the DFT results displayed in Fig. 4. This small energy is gained through the destruction of four of the eight bonds that the impurity has at $Z=0$ to create four stronger ones. As this energy is gained through the rebonding involving the whole 46 valence orbitals of the FeCl_8^{7-} complex, this simple fact stresses the subtle origin of the off-center mechanism.

Searching to gain better insight on this issue, the orbital energy is portrayed (Fig. 5) as a function of Z for some relevant valence levels of the FeCl_8^{7-} complex. In addition to ligand levels, the evolution of antibonding t_{2g} levels that are partly filled is also depicted in Fig. 5. Under a C_{4v} symmetry, there is a splitting between $e(xz, yz)$ and $b_2(xy)$ levels emerging from the antibonding t_{2g} in O_h (Fig. 2). In Fig. 5, the Z dependence of unoccupied $e(4p_x, 4p_y)$ orbitals arising from the $4p$ shell of free Fe^+ is also plotted. It can be expected that when Fe^+ moves significantly upward bonding is established mainly with the e and b_2 orbitals of the top ligands, while the ionic negative charge of the bottom ligands increases by $0.02e$, as well reflected in the orbital energies variation of Fig. 5. It can be noted in Fig. 5 that for $Z > 0.5 \text{ \AA}$, the mainly top and bottom orbitals are separated. The former orbitals have a smaller energy than the latter ones as a result of being in the neighborhood of the positive Fe^+ ion. Moreover, as could be anticipated, bonding effects appear to be more important on the top ligands than on the bottom ones. The energy variation of antibonding $e(xz, yz)$ and $b_2(xy)$ levels along the Z coordinate (Fig. 5) also reflects the influence of $V_C(Z)$ upon the energy of such levels. It should be noted that $V_C(Z)$ acts against the motion of the positive iron ion as a whole but favors an energy decrease of mainly $3d$ levels.

Together with the bonding-antibonding mechanism of occupied e and b_2 levels, attention should be paid to the behav-

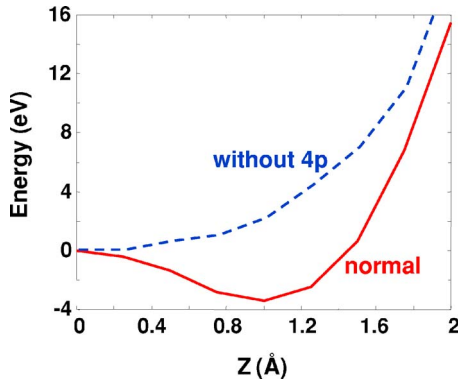


FIG. 6. (Color online) Solid line: Ground-state total energy, $E(Z)$, of SrCl₂:Fe⁺ obtained in a normal SCCEH calculation for different values of the Z coordinate. Dashed line: Ground-state total energy, $E(Z)$, of SrCl₂:Fe⁺ obtained in a normal for a SCCEH calculation where the $4p(\text{Fe})$ orbital has been removed from the basis set.

ior displayed by the *unoccupied* $e(4p_x, 4p_y)$ orbitals in Fig. 5. It can first be noted that the energy of such unoccupied orbitals increases following the distortion parameter Z . Moreover, this fact is accompanied by the energy decrease of other partly or fully occupied e levels lying below. To explore the importance of unoccupied $4p$ orbitals in the off-center motion of Fe⁺ in SrCl₂, SCCEH calculations have also been performed. In addition to normal SCCEH calculations, results have also been derived removing the $4p$ orbitals from the basis set (Fig. 6). It can first be noted that normal SCCEH calculations are able to reproduce (albeit qualitatively) the main features of the off-center instability observed for SrCl₂:Fe⁺. By contrast, when the $4p$ orbitals are removed from the basis set, $[\partial^2 E(Z)/\partial Z^2]_{Z=0}$ is found to be positive and the on-center position to be stable. We have verified that if the $4s$ orbital of Fe⁺ is suppressed from the basis set, the off-center instability is still encountered in SCCEH calculations. This result is not surprising, because linear vibronic coupling between $3d$ and $4s$ levels of Fe⁺ via the t_{1u} mode is forbidden due to parity restrictions. This simple reasoning can shed light on the different role played by the $4s$ and $4p$ orbitals of Fe⁺ with regard to the off-center instability.

The present results emphasize the important role played by the $4p$ orbitals of monovalent $3d$ ions regarding the off-

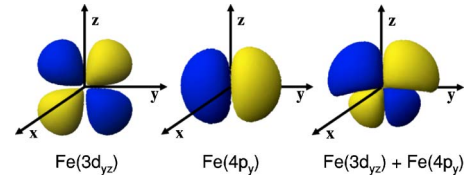


FIG. 7. (Color online) Qualitative picture describing the hybridization between $3d_{yz}$ and $4p_y$ orbitals of Fe.

center instabilities in fluorite-type lattices. It is worth noting that this mechanism has not been considered in previous studies,^{23,24} and its relevance likely decreases on passing from monovalent to divalent ions. In fact, in the latter cases, the separation between the $3d$ and $4p$ levels lies above 10 eV, being equal to 15 eV for free Cu²⁺.⁴⁵ The importance of the hybridization between the $3d_{yz}$ and $4p_y$ orbitals is pictured in Fig. 7. The main result of such hybridization is that the electronic density moves from the lower part to the upper parts. Through this mechanism, the bonding with top ligands is favored, while bottom ligands are progressively disconnected.

Relevant information on the two rebonding (or pseudo-Jahn-Teller) mechanisms contributing to the off-center distortion of Fe⁺ in SrCl₂ can be obtained by means of DFT calculations performed for *different* electronic configurations (Table I). Following previous works on d^9 impurities,^{23,24} in the first step, calculations have been made for the artificial $(3z^2 - r^2)^{7/5}(x^2 - y^2)^{7/5}xz^{7/5}yz^{7/5}xy^{7/5}$ configuration with the seven electrons equally distributed into the five $3d$ orbitals. It can be observed in Table I that, in contrast to the results for d^9 impurities, the off-center distortion is not quenched for this average configuration, although the well depth is smaller than for the actual ground state. In the second step, the influence of the xy occupation, but keeping the $e_g^{4,3}t_{2g}^3$ ground-state configuration (in cubal symmetry), has been explored. As shown in Table I the Fe⁺ impurity remains *on center* when the xy orbital is fully occupied $[(3z^2 - r^2)^2(x^2 - y^2)^2xz^{0.5}yz^{0.5}xy^2]$ configuration, while the off-center excursion is very reinforced when the xy level is empty. These results already show evidence for the crucial role of the xy orbital in the off-center motion of Fe⁺. It is worth noting that on passing from the $(3z^2 - r^2)^2(x^2 - y^2)^2xz^{0.5}yz^{0.5}xy^2$ to the $(3z^2 - r^2)^1(x^2 - y^2)^0xz^2yz^2xy^2$ configuration [where *both* xy

TABLE I. Depth of the energy wells and equilibrium value of the off-center distortion, Z_0 , obtained from DFT calculations for different C_{4v} electronic configurations, including the ground state (GS). The corresponding cubal (O_h) configurations are also shown.

| C_{4v} electronic configuration | O_h configuration | Energy (eV) | Z_0 (Å) |
|---|---------------------------|-------------|-----------|
| $a_1(z^2)^2b_1(x^2 - y^2)^2e(xz, yz)^2b_2(xy)^1$ / (GS) | $e_g^{4,3}t_{2g}^3$ | 0.28 | 1.31 |
| $a_1(z^2)^{7/5}b_1(x^2 - y^2)^{7/5}e(xz, yz)^{14/5}b_2(xy)^{7/5}$ | $e_g^{14/5}t_{2g}^{21/5}$ | 0.16 | 1.13 |
| $a_1(z^2)^2b_1(x^2 - y^2)^2e(xz, yz)^1b_2(xy)^2$ | $e_g^{4,3}t_{2g}^3$ | 0 | 0 |
| $a_1(z^2)^1b_1(x^2 - y^2)^0e(xz, yz)^4b_2(xy)^2$ | $e_g^{1,6}t_{2g}^4$ | 0.07 | 0.97 |
| $a_1(z^2)^2b_1(x^2 - y^2)^2e(xz, yz)^3b_2(xy)^0$ | $e_g^{4,3}t_{2g}^3$ | 1.30 | 1.59 |
| $a_1(z^2)^2b_1(x^2 - y^2)^1e(xz, yz)^4b_2(xy)^0$ | $e_g^{3,4}t_{2g}^4$ | 1.73 | 1.56 |
| $a_1(z^2)^2b_1(x^2 - y^2)^0e(xz, yz)^4b_2(xy)^1$ | $e_g^{2,5}t_{2g}^5$ | 1.01 | 1.57 |
| $a_1(z^2)^2b_1(x^2 - y^2)^1e(xz, yz)^3b_2(xy)^1$ | $e_g^{5,4}t_{2g}^4$ | 0.62 | 1.48 |

and $e(xz, yz)$ levels are fully occupied], a small off-center instability is recovered. Thus, result shows that an increase in the population of $e(xz, yz)$ levels favors the off-center motion indeed. Calculations carried out for other electronic configurations in Table I do support that the off-center instability is favored by decreasing the xy population and increasing the population of $e(xz, yz)$ levels. In particular, the biggest effect is found for the $(3z^2 - r^2)^2(x^2 - y^2)^1xz^2yz^2xy^0$ configuration such as displayed in Table I.

IV. FINAL REMARKS

From the present analysis, the off-center motion is driven by vibronic coupling with excited states that decrease the ground-state energy when Z increases. Therefore, this pseudo-Jahn-Teller interaction can take place even if the ground state is not degenerate. Thus, this result is quite different from the result found in the Jahn-Teller effect where the existence of electronic degeneracy implies that the geometry associated with adiabatic minima is *necessarily* distorted. In the present case, this statement is no longer true as the existence of a spontaneous instability at $T=0$ K requires that $[\partial^2 E(Z) / \partial Z^2]_{Z=0} < 0$.

The results of this work show the importance of DFT calculations for gaining a better insight into the off-center phenomenon. Such calculations allow us to explore the big off-center motion in $\text{SrCl}_2:\text{Fe}^+$ in a *wide range* of the distortion parameter, Z , and thus when the perturbative expansion used in vibronic models is no longer applicable. On the other hand, the use of calculations for different electronic configurations has been shown to convey crucial information on orbitals mainly involved in the pseudo-Jahn-Teller instability and the associated rebonding effects.

As previously indicated, the off-center phenomenon observed in $\text{SrCl}_2:\text{Fe}^+$ cannot be reproduced through expensive CASPT2 calculations. In this kind of calculations the $3d$, $4s$, and $4p$ levels coming from Fe^+ are included in the active space, while the rest of the valence electrons are correlated through a many-body second-order perturbation method. Similar CASPT2 calculations performed in the $\text{CaF}_2:\text{Ni}^+$

center were also unable to reproduce the experimentally observed⁵ off-center distortion. It is worth noting that the inclusion of all bonding orbitals in the active space would dramatically increase the cost of the calculations. Therefore, the subtle instability in some fluorite-type lattices doped with d^9 and d^4 ions is actually a challenge for wave-function-based calculations. This remarkable difference between DFT and CASPT2 calculations may reflect, that in the latter method, the ligand levels are not treated on the same footing as the mainly $3d$, $4s$, and $4p$ levels from the impurity. However, such levels are deeply involved in the rebonding process that plays a key role in the off-center phenomenon. It is worth noting that rebonding has been shown to play a minor role in the case of the $E \otimes e$ Jahn-Teller effect. Nevertheless, some sizable influence of pseudo-Jahn-Teller interactions on the barrier among equivalent minima has recently been demonstrated.⁴⁶

It was pointed out^{23,24} early that in fluorite-type lattices, the Coulomb barrier $qeV_C(Z)$ increases when the lattice parameter decreases, and when a monovalent $3d$ ion is replaced by an other divalent one. According to this qualitative idea, there is an off-center instability in $\text{CaF}_2:\text{Ni}^+$ but not in $\text{CaF}_2:\text{Cu}^{2+}$ and $\text{CaF}_2:\text{Ag}^{2+}$. The present results strongly suggest that the vibronic admixture with *unoccupied* $4p$ orbitals can also help the existence of an off-center motion in $\text{CaF}_2:\text{Ni}^+$ well observed through EPR and ENDOR measurements.⁵

In conclusion, the present work stresses the usefulness of DFT calculations on relatively small clusters for gaining a better insight into the local instabilities around an impurity. In this domain, a surprising instability has been observed^{47,48} in $\text{BaF}_2:\text{Mn}^{2+}$ where the cube formed by fluorine ligands undergoes a slight $O_h \rightarrow T_d$ distortion below about 45 K. Further work along this subtle issue is now under way.

ACKNOWLEDGMENTS

Partial support by the Spanish Ministerio de Ciencia y Tecnología under Project No. MAT2005-00107 is acknowledged.

¹H. Bill, Phys. Lett. **44A**, 101 (1973).

²M. Moreno, An. Fis. (1968-1980) **70**, 261 (1974).

³H. Bill, in *The Dynamical Jahn-Teller Effect in Localized Systems*, edited by Yu. E. Perlin and M. Wagner (Elsevier, Amsterdam, 1984), p. 709.

⁴M. D. Glinchuk, in *The Dynamical Jahn-Teller Effect in Localized Systems*, edited by Yu. E. Perlin and M. Wagner (Elsevier, Amsterdam, 1984), p. 819.

⁵P. Studzinski, J. Casas Gonzalez, and J. M. Spaeth, J. Phys. C **17**, 5411 (1984).

⁶R. Alcalá, R. Cases, and P. J. Alonso, Phys. Status Solidi B **135**, K63 (1986).

⁷D. S. McClure and S. C. Weaver, J. Phys. Chem. Solids **52**, 81 (1991).

⁸P. B. Oliete, V. M. Orera, and P. J. Alonso, Phys. Rev. B **53**, 3047

(1996).

⁹V. Lefevre, A. Monnier, M. Schnieper, D. Lovy, and H. Bill, Z. Phys. Chem. **200**, 265 (1997).

¹⁰P. B. Oliete, V. M. Orera, and P. J. Alonso, Appl. Magn. Reson. **15**, 155 (1998).

¹¹S. K. Hoffmann and V. A. Ulanov, J. Phys.: Condens. Matter **12**, 1855 (2000).

¹²V. A. Ulanov, M. Krupski, S. K. Hoffmann, and M. M. Zaripov, J. Phys.: Condens. Matter **15**, 1081 (2003).

¹³A. M. Stoneham, in *Theory of Defects in Solids: Electronic Structure of Defects in Insulators and Semiconductors* (Oxford University Press, New York, 2001).

¹⁴R. Kadono, in *Atom Tunneling Phenomena in Physics, Chemistry and Biology* (Springer, Berlin, 2004).

¹⁵H. R. Schober and A. M. Stoneham, Phys. Rev. Lett. **60**, 2307

- (1988).
- ¹⁶R. Ramirez, C. P. Herrero, E. Artacho, and F. Yndurain, *J. Phys.: Condens. Matter* **9**, 3107 (1997).
- ¹⁷A. M. Stoneham, *Phys. Rev. Lett.* **84**, 4777 (2000).
- ¹⁸M. J. Shaw, P. R. Briddon, J. P. Goss, M. J. Rayson, A. Kerridge, A. H. Harker, and A. M. Stoneham, *Phys. Rev. Lett.* **95**, 105502 (2005).
- ¹⁹I. B. Bersuker, *Ferroelectrics* **164**, 5 (1995).
- ²⁰I. B. Bersuker, in *Electronic Structure and Properties of Transition Metal Compounds* (Wiley, New York, 1996).
- ²¹K. Leung, *Phys. Rev. B* **65**, 012102 (2001).
- ²²A. R. Akbarzadeh, L. Bellaiche, K. Leung, J. Iñiguez, and D. Vanderbilt, *Phys. Rev. B* **70**, 054103 (2004).
- ²³J. A. Aramburu, P. García-Fernández, M. T. Barriuso, and M. Moreno, *Phys. Rev. B* **67**, 020101(R) (2003).
- ²⁴P. García-Fernández, J. A. Aramburu, M. T. Barriuso, and M. Moreno, *Phys. Rev. B* **69**, 174110 (2004).
- ²⁵V. A. Ulanov, M. M. Zaripov, V. A. Shustov, and I. I. Fazlizhanov, *Phys. Solid State* **40**, 408 (2001).
- ²⁶M. M. Zaripov and V. A. Ulanov, *Sov. Phys. Solid State* **30**, 896 (1988).
- ²⁷S. V. Nistor, M. Stefan, and D. Schoemaker, *Phys. Status Solidi B* **214**, 229 (1999).
- ²⁸D. Ghica, S. V. Nistor, H. Vrielinck, F. Callens, and D. Schoemaker, *Phys. Rev. B* **70**, 024105 (2004).
- ²⁹J. R. Pilbrow, in *Transition Ion Electron Paramagnetic Resonance* (Clarendon, Oxford, 1990), p. 134.
- ³⁰M. Moreno, J. A. Aramburu, and M. T. Barriuso, *Phys. Rev. B* **56**, 14423 (1997).
- ³¹G. te Velde, F. M. Bickelhaupt, E. J. Baerends, C. Fonseca Guerra, S. J. A. van Gisbergen, J. G. Snijders, and T. Ziegler, *J. Comput. Chem.* **22**, 931 (2001).
- ³²S. H. Vosko, L. Wilk, and M. Nusair, *Can. J. Phys.* **58**, 1200 (1980).
- ³³A. D. Becke, *Phys. Rev. A* **38**, 3098 (1988); C. Lee, W. Yang, and R. G. Parr, *Phys. Rev. B* **37**, 785 (1988).
- ³⁴R. G. Parr and W. Yang, in *Density Functional Theory in Atoms and Molecules* (Oxford University Press, New York, 1989).
- ³⁵C. A. Daul, K. G. Doclo, and A. C. Stückl, in *Recent Advances in Density Functional Methods, Part II*, edited by Delano Chong (World Scientific, Singapore, 1997).
- ³⁶J. A. Aramburu, M. Moreno, K. Doclo, C. Daul, and M. T. Barriuso, *J. Chem. Phys.* **110**, 1497 (1999).
- ³⁷M. Atanasov, C. A. Daul, and C. Rauzy, *Chem. Phys. Lett.* **367**, 737 (2003).
- ³⁸A. D. Becke, *J. Chem. Phys.* **98**, 5648 (1993).
- ³⁹M. J. Frisch *et al.*, GAUSSIAN 98, Gaussian, Inc., Pittsburgh, PA, 1998.
- ⁴⁰B. O. Roos, in *New Challenges in Computational Quantum Chemistry*, edited by R. Broer, P. J. C. Aerts, and P. S. Bagus (Groningen, The Netherlands, 1994), p. 12.
- ⁴¹K. Andersson, M. Barysz, A. Bernhardsson, M. R. A. Blomberg, D. L. Cooper, M. P. Fülscher, C. de Graaf, B. A. Hess, G. Karlström, R. Lindh, P.-Å. Malmqvist, T. Nakajima, P. Neogrády, J. Olsen, B. O. Roos, B. Schimmelpfennig, M. Schütz, L. Seijo, L. Serrano-Andrés, P. E. M. Siegbahn, J. Stålring, T. Thorsteinsson, V. Veryazov, and P.-O. Widmark, MOLCAS Version 5.4 K (Lund University, Sweden, 2002).
- ⁴²L. Seijo and Z. Barandiarán, in *Computational Chemistry: Reviews of Current Trends*, edited by J. Leszczynski (World Scientific, Singapore, 1999).
- ⁴³G. Pacchioni, F. Frigoli, D. Ricci, and J. A. Weil, *Phys. Rev. B* **63**, 054102 (2000); C. Sousa, C. de Graaf, F. Illas, M. T. Barriuso, J. A. Aramburu, and M. Moreno, *Phys. Rev. B* **62**, 13366 (2000); C. Sousa, C. de Graaf, and F. Illas, *Phys. Rev. B* **62**, 10013 (2000); L. Hozoi, A. H. de Vries, and R. Broer, *Phys. Rev. B* **64**, 165104 (2001); L. Hozoi, C. Presura, C. de Graaf, and R. Broer, *Phys. Rev. B* **67**, 035117 (2003).
- ⁴⁴J. H. Ammeter, A. B. Burgi, J. C. Thibeault, and R. Hoffman, *J. Am. Chem. Soc.* **100**, 3686 (1978).
- ⁴⁵C. E. Moore, *Natl. Stand. Ref. Pat. Ser. Natl. Bureau Stand.*, No. 35 (U.S. GPO, Washington, D.C., 1971).
- ⁴⁶P. García-Fernández, I. B. Bersuker, J. A. Aramburu, M. T. Barriuso, and M. Moreno, *Phys. Rev. B* **71**, 184117 (2005).
- ⁴⁷A. G. Badalyan, P. G. Baranov, V. S. Vikhnin, and V. A. Khramtson, *JETP Lett.* **44**, 110 (1986).
- ⁴⁸H. Soethe, V. A. Vetrov, and J. M. Spaeth, *J. Phys.: Condens. Matter* **4**, 7927 (1992).